Scale-dependent miscibility of polylactide and polyhydroxybutyrate

Please check the document version of this publication:

• A submitted manuscript is the version of the article upon submission and before peer-review. There can be important differences between the submitted version and the official published version of record. People interested in the research are advised to contact the author for the final version of the publication, or visit the DOI to the publisher's website.
• The final author version and the galley proof are versions of the publication after peer review.
• The final published version features the final layout of the paper including the volume, issue and page numbers.

[Link to publication](#)

Scale-Dependent Miscibility of Polylactide and Polyhydroxybutyrate: Molecular Dynamics Simulations

Artyom D. Glova[a], Stanislav G. Falkovich[a], Daniil I. Dmitrienko[b], Alexey V. Lyulin[c], Sergey V. Larin[a], Victor M. Nazarychev[a], Mikko Karttunen[a,d], and Sergey V. Lyulin[a,b,]*

[a]Institute of Macromolecular Compounds, Russian Academy of Sciences, Bolshoj pr. V.O., 31, 199004 St. Petersburg, Russia

[b]Faculty of Physics, Saint-Petersburg University, Ulyanovskaya str. 1, Petrodvorets, 198504 St. Petersburg, Russia

[c]Theory of Polymers and Soft Matter Group, Technische Universiteit Eindhoven, PO Box 513, 5600 MB, Eindhoven, The Netherlands

[d] Department of Chemistry and Department of Applied Mathematics, Western University, 1151 Richmond St, London, Ontario, Canada, N6A 5B7

ABSTRACT: Miscibility of polylactide (PLA) and polyhydroxybutyrate (PHB) is studied by the microsecond atomistic molecular-dynamics (MD) simulations for the first time. The model and the simulation protocol were confirmed through comparison of the glass transition temperature (T_g) with experimental data. It was established that PLA and PHB are miscible on the basis of the

Flory–Huggins theory. Analysis of the mobilities of PLA and PHB subchains revealed that the blends have two transitions to a glassy state at the length scale of a few Kuhn segments, which is in line with the predictions of the self-concentration model. At the same time at the larger length scale, a single transition to a glassy state was observed suggesting scale-dependence of PLA and PHB miscibility. This scale-dependence was confirmed through the evaluation of the interchain pair correlation functions.

I. INTRODUCTION

Polylactide (PLA) and polyhydroxybutyrate (PHB) are thermoplastic semi-crystalline polyesters.[1,2] Their key properties are biodegradability, biocompatibility, and low toxicity making them promising alternatives to polymers synthesized from the petroleum products.[3] As pointed out by Arrieta et al. in their extensive review of PLA-PHB blends,[4] PLA is currently the most commonly used polymer in food packing but its mechanical properties remain problematic. As a pure substance, PHB is brittle but has high Young's modulus.[5] Since PLA-PHB blends are biocompatible, they have received a lot of attention as a potential route to food packaging materials with improved mechanical properties. For example, Zhang and Thomas[6] showed that the tensile stress increases from 25.5±3.0 MPa for pure PLA to 32.2±3.9 MPa in 75%:25% PLA-PHB blend, and Lai et al.[7] prepared blends composed of high molecular weight PLA and low molecular weight PHB and found that the breaking elongation of PLA can be significantly increased from 7.2 % to 227 % by the addition of PHB oligomers.

In order for the polymer blend to have improved mechanical characteristics compared to those of the pure components, the polymers species must be miscible, i.e. form a uniform single-phase mixture.[6,8] Generally, polymer blends can be divided into three categories: miscible, semi-miscible (or partially miscible), and immiscible blends.[9] One of the widely used experimental

characteristics to distinguish polymer-polymer miscibility is the glass transition temperature, T_g. A blend of miscible polymers exhibits a single T_g, as well as a single homogeneous phase. Two distinct T_g values arising from two phase-segregated components are often interpreted as an indicator of immiscibility.[9–11] A blend of semi-miscible polymers is also characterized by two glass transition temperatures, but their values are shifted from the values of the corresponding pure components.[10,11]

An alternative view has been proposed by Lodge and McLeish.[12] According to their self-concentration model, chain connectivity of polymers leads to an increased local concentration of monomers in blends compared to an average bulk concentration. For this reason, one should normally expect two glass transitions in any single-phase polymer blend. Thus, it was suggested that the presence of two distinct T_g values cannot be used as a reliable criterion of immiscibility and semi-miscibility.[13] The matter is, however, complex since it is difficult to determine how exactly the different components contribute to the behavior of the blend.[14,15]

Previous studies have established that miscibility of blends depends on the chemical structures and the molecular weights of the components.[9] In terms of their chemical structures, PLA and PHB are quite similar. The main difference between PHB and PLA monomers is an extra methylene group within the PHB backbone, see Figure 1. Thus, one can expect them to be miscible.[16] However, the dependence of miscibility on the molecular weight of PLA and PHB is not straightforward. Some authors have reported that PLA is miscible with low molecular weight PHB (M_w < 30 kg/mol),[11,17–19] while others found the miscibility of PHB with low molecular weight PLA (M_w < 18 kg/mol).[20–23] For PLA-PHB blends in which molecular weight exceeds 60 kg/mol, contradicting results have been found: several authors have reported that high

molecular weight PLA and PHB are miscible[16,17,24–27], whereas the others stated that they are immiscible[6,8,10,18,20,21,28–31].
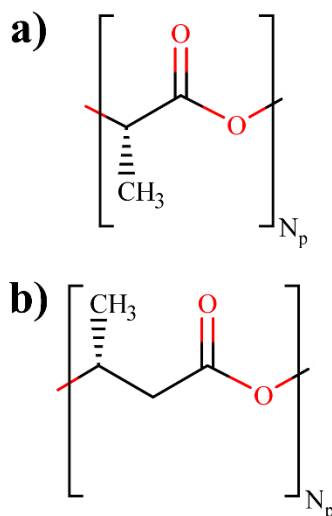

Figure 1. Chemical structures of the a) PLA and b) PHB monomers.

Complementary to experiments, the atomistic MD simulations provide an efficient tool to investigate miscibility of polymers. They have the ability to supply detailed atomistic level information on structural, thermal, and dynamic properties of blends. Therefore, using atomistic simulations to evaluate miscibility and the dominant physical mechanisms has attracted a continuing attention of researchers.[32–43]

MD simulations have been used to study the glass transition to predict miscibility of blended polymers.[33,35–37] It has been established that interchain pair correlation functions may reflect structural properties of samples which can directly be related to miscibility.[32,34,35,38,39,42] In addition, the Flory–Huggins theory has been applied to shed light on the possibility for some polymers to be miscible.[32–41,43] Typically, two criteria for miscibility are utilized when using the Flory–Huggins approach: 1) for a miscible composition, the interaction parameter χ has to be lower than some critical value χ_{cr} (see Supporting Information for the details) and 2) the

solubility parameters (δ) have to be close enough to each other. According to Coleman et al.[44], for weakly interacting polymers such as PLA and PHB this difference should not exceed 2 $(J/cm^3)^{0.5}$.

Majority of the existing atomistic simulations of blends are, however, relatively short and the simulation times do not exceed several nanoseconds.[32–43] Our previous study[45] has shown that the simulation times required for a proper equilibration of polymer samples can reach microseconds.

In this study, we report the results of the first MD study of miscibility for the blends of the low molecular weight PLA and PHB. To ensure proper equilibration, each of the production simulations was carried out for 5 µs to allow for careful investigation of the various miscibility criteria. We examined whether PLA and PHB are miscible via the Flory-Huggins theory and via the change of system density upon the transition from a melt to a glassy state. We also addressed how the physical properties of blends depend on the length scale by studying the influence of temperature on chain mobility. The structural properties of the blends were evaluated using interchain pair correlation functions. The main result of this study is that miscibility of the blends is scale-dependent: they are semi-miscible within the length of a few Kuhn segments although being miscible at the larger length scale.

II.   MODEL AND SIMULATION METHOD

Five systems with different weight fractions of PHB (0%, 23%, 49%, 74%, and 100%) in the blends were considered. Each simulated system consisted of 20 polymer chains. The degree of polymerization, N_p, for both PLA and PHB was set to 150. This value yields molecular weights of approximately 11 kg/mol and 13 kg/mol for PLA and PHB, respectively. From the standpoint of experimental data, such weights are relatively low and the miscibility of the components is

expected.[11,17–20,22,23] However, the value of molecular weight for PLA is large enough as it corresponds to the polymer regime in the Fox-Flory dependence for the glass transition temperature.[46] Parameters of the simulated blends are listed in Table 1.

Table 1. Details of the simulated blends.

System №	Degree of polymerization of PLA and PHB chains	Number of chains		Weight fraction, %		Length of the simulation box (cubic) side, nm	Number of atoms
		PLA	PHB	PLA	PHB		
1	150	20	0	100	0	7.0	27060
2	150	16	4	77	23	7.1	28860
3	150	11	9	51	49	7.3	31110
4	150	6	14	26	74	7.4	33360
5	150	0	20	0	100	7.5	36060

The General AMBER Force Field (GAFF)[47] was used for bonded and non-bonded interactions. GAFF has previously been successfully applied in the simulations of thermal, dynamic, and structural properties of organic molecules and polymer systems.[48–52] Lorentz-Berthelot mixing rules were used to describe van der Waals interactions as required by the GAFF force field.[53] The topologies of the PLA and PHB monomer units were generated with the aid of the ACPYPE tool which is a wrapper for the antechamber module of Ambertools.[54,55] The partial atomic charges were calculated using the Gaussian 09 software by the HF/6-31G*(RESP) method.[56] Such an approach is the standard for the parameterization of the GAFF force field[47] and has been successfully used in our previous simulations.[57,58] The force field parameters as well as atomic coordinate files for PLA and PHB chains used in the present study are provided in Supporting Information.

The computer simulations were carried out following the methodology developed for atomistic modeling of bulk and composite systems in our previous studies.[45,57,59–68] Initially, we filled a periodic cubic box with a chosen amount of PLA and PHB chains at a sufficiently low density. Having constructed the initial configuration, we performed energy minimization using the method of steepest descents.[69] Then, the simulations were carried out in the NpT ensemble for 10 ns at a temperature of 550 K and a pressure of 50 bar, to reach the system density close to the experimental conditions.[1,2] After this compression, the production MD simulations were carried out for 5 μs at a constant pressure of 1 bar and a temperature of 550 K. This is above the PLA and PHB melting temperature (T_m) which is approximately 450 K.[1,2] The use of such a high temperature allowed us to accelerate the equilibration and to study properties of the blends in a melt.[70]

The simulations were performed using the open source Gromacs 5.1.1 package.[69] The velocity-Verlet algorithm was utilized to integrate the equations of motion and the time step was set to 2 fs.[63] The Berendsen thermostat and barostat were applied to keep the temperature and pressure constant.[71] The time relaxation constants were set to $\tau_T = 0.1$ ps for the thermostat and $\tau_P = 1$ ps for the barostat.[65] The long-range electrostatic interactions were taken into account by the particle-mesh Ewald (PME) method with the real space cutoff distance set to 1 nm.[72,73] The van der Waals interactions were truncated at 1 nm.[59]

III.   RESULTS AND DISCUSSION

Equilibration of systems. Achieving equilibration is crucial for reliability of MD simulations.[45] It has been recently shown that even at temperatures significantly exceeding T_g, MD simulations at time-scales up to microseconds may be required to reach equilibrium in polymer systems.[45,66,67] To estimate the time necessary for the equilibration, we calculated the

time dependence of the radius of gyration R_g and the end-to-end distance $H_{end-to-end}$ of PLA and

PHB chains, Figure 2. The curves in Figure 2 are fitted by the

function $y(t) = A + B \cdot (1 - \exp(-t/\tau))$, where A, B and τ are the fitting parameters. The fits

show that the characteristic time τ is in the range of 100–500 ns, depending on the system (see

Supporting Information, Table S1). We chose the first microsecond as the time-span for

equilibration. The last four microseconds were considered as equilibrated and were used in data

analysis. The mean equilibrium values of $H_{end-to-end}$ and R_g were 8.4 ± 1.0 nm and 3.4 ± 0.4 nm,

respectively. They turned out to be equal for both PLA and PHB within the margin of error in all

the blends.
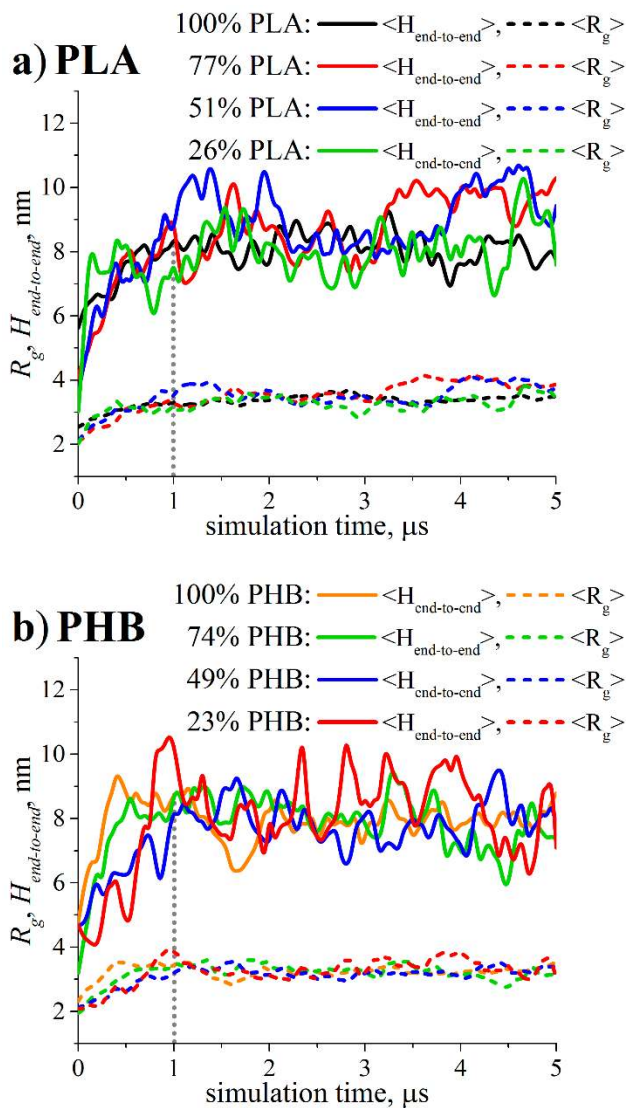
Figure 2. Time dependence of the radius of gyration R_g and the end-to-end distance $H_{end-to-end}$ for a) PLA and b) PHB chains for different systems. The dotted lines show the equilibration time of 1 μs.

In analogy with a recent study[74], we calculated the dimensionless characteristic ratios C_∞ for both PLA and PHB chains in the blends to verify the quality of the equilibration. The technical details are provided in Supporting Information. In pure systems, the C_∞ value for the PLA

chains was equal to 10.2 ± 0.2, while for the PHB chains we determined $C_\infty^{PHB} = 5.8 \pm 0.1$. In blends, the values of C_∞^{PLA} and C_∞^{PHB} were almost identical to those in the pure systems, indicating that the inherent stiffness of the chains does not change upon blending. The characteristic ratios are qualitatively comparable with the results of 11.8 for PLA and 6.1–6.3 for PHB obtained using light scattering experiments.[75,76] The observed small quantitative differences may stem from the short length of the chains in our simulations. Nevertheless, this confirms that our systems are well-equilibrated. Using the characteristic ratios, we calculated the persistence lengths $l_p^{PLA} = 0.8 \pm 0.1$ nm and $l_p^{PHB} = 0.5 \pm 0.1$ nm for PLA and PHB, respectively. At the same time, data from Refs. 75 and 76 gives $l_p^{PLA} = 0.9$ nm and $l_p^{PHB} = 0.5$ nm, i.e. our simulations reproduce the difference in stiffness between PLA and PHB well. This validates the force field and the model.

We additionally verified the equilibration time using monomer displacements. To this end, we measured the mean-square displacements (MSD) of the centers of masses of the monomers as

$$\left\langle \Delta r^2(\Delta t) \right\rangle = \left\langle \left(\vec{r}(t + \Delta t) - \vec{r}(t) \right)^2 \right\rangle \tag{1}$$

where $\left\langle ... \right\rangle$ denotes an average over the simulation time t and over all monomers.

The monomer displacement of a distance comparable with the chain size implies that the chain conformations are able to change completely.[45] Figure 3 demonstrates the MSD together with the values of R_g^2 and the squared Kuhn segment length $\left(2l_p \right)^2$. As the figure shows, the PLA and PHB monomers move over distances comparable with the polymer coil size in less than 400 ns. It can thus be assumed that during this simulation time the systems forget their initial configurations as well as lose correlations (memory). Therefore, we determined that 1 μs, which well exceeds 400 ns, is pertinent for the equilibration of the blends.
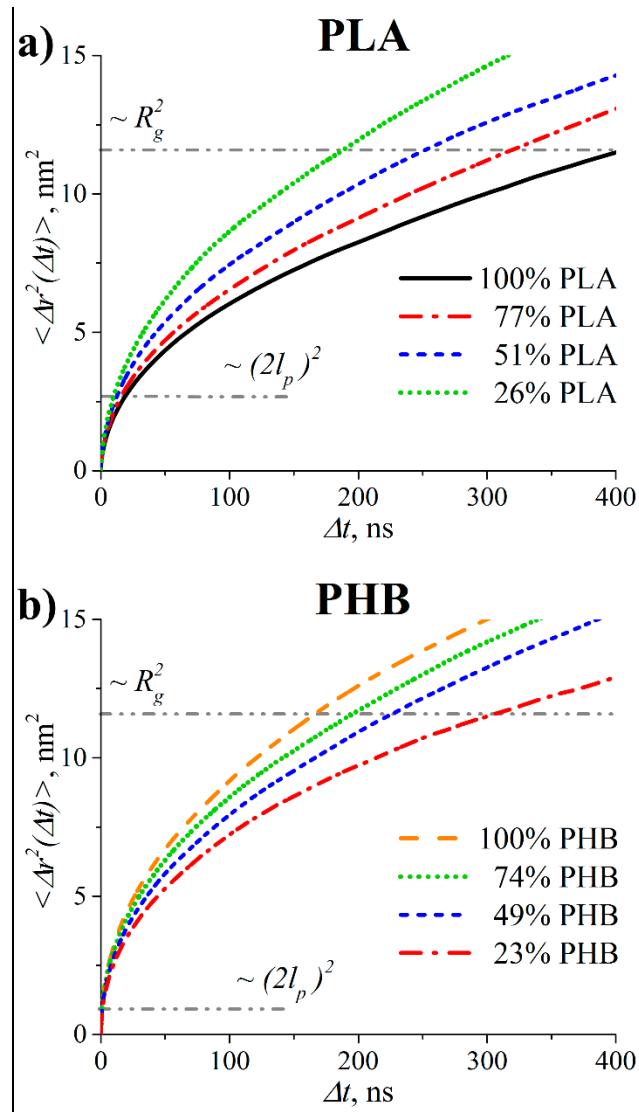
Figure 3. The mean-square displacement of the centers of mass $\left\langle \Delta r^2(\Delta t) \right\rangle$ of the a) PLA and b) PHB monomers for different systems. The dash-dot-dot lines show the squared radius of gyration R_g^2 and the Kuhn segment $\left(2l_p \right)^2$.

Visual analysis. We now focus on the miscibility of PLA and PHB. Figure 5 shows typical snapshots of PLA and PHB blends at the end of the production runs at 550 K. They clearly show the absence of the phase separation of chains into two homogeneous regions.
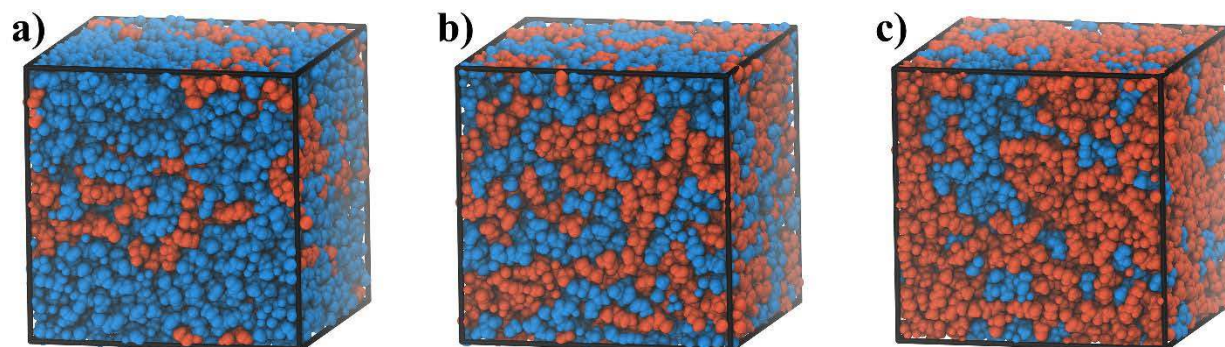

Figure 4. Snapshots of PLA and PHB blends at the end of the simulations at $T = 550$ K. PLA and PHB chains are colored in blue and red, respectively. PHB weight fractions: a) 23%, b) 49%, and c) 74%.

Application of the Flory–Huggins theory. By utilizing the simulation data one can study polymer-polymer miscibility with the Flory–Huggins theory.[9] Two polymers are miscible when the change in the Gibbs free energy of blending $\Delta G = \Delta H - T\Delta S < 0$, where ΔH and ΔS are the enthalpic and entropic terms, and T is the temperature. Since polymer chains have small entropy, miscibility depends mainly on the enthalpic term. To establish the miscibility of polymers in MD simulations, two characteristics were measured:[32–41] the difference in the Hildebrand solubility parameter for pure components $\Delta\delta$ and the Flory–Huggins interaction parameter χ. As usual,[32–41] we calculated the cohesive energy densities for the pure PLA and PHB in order to estimate their solubility parameters. The values of χ for the blends were calculated through the internal energy change upon mixing following Refs. 32, 43; the Supporting Information provides the details of calculations of solubility and Flory–Huggins

parameters. The results are shown in Table 2 together with experimental data[77,78] and the recent results from the Hoftyzer–Van Krevelen (HVK) group contribution method[79].

Table 2. The reported experimental[77,78] δ^{exp} and Hoftyzer–Van Krevelen δ^{HVK} solubility parameters[79]. The Hildebrand solubility parameters δ^{sim} and the Flory–Huggins interaction parameters χ were calculated from the present MD simulations. Note that the MD simulation data is at $T = 550$ K, while the reference data is at room temperature.

Weight fraction, %		δ^{sim}, (J/cm^3)$^{0.5}$	δ^{exp}, (J/cm^3)$^{0.5}$	δ^{HVK}, (J/cm^3)$^{0.5}$	χ
PLA	PHB				
100	0	14.8 ± 0.1	19-20.5	20.8	-
77	23	14.6 ± 0.1			0.0 ± 0.4
51	49	14.4 ± 0.1			0.2 ± 0.3
26	74	14.2 ± 0.1			0.2 ± 0.3
0	100	14.0 ± 0.1	19.8	19.8	-

It is seen that the solubility parameters δ^{sim} calculated from the MD simulation data were 14.8 ± 0.1 (J/cm^3)$^{0.5}$ for pure PLA and 14.0 ± 0.1 (J/cm^3)$^{0.5}$ for pure PHB. For blends, the δ^{sim} lie between these values and decrease with increasing PHB fraction. The quantitative discrepancy in the solubility parameters δ^{sim} compared to δ^{exp} and δ^{HVK} may stem from the fact that the present simulations were carried out at a high temperature of 550 K, while the reference values were obtained at room temperature. Since the solubility parameter δ is defined by molar volume V_M and cohesive energy E_{coh} of the system as $\delta = (E_{coh} / V_M)^{0.5}$, the question that arises is what lowers the solubility – the molar volume or the cohesive energy? To answer this question, we calculated the values of V_M, E_{coh}, and δ at T=300K using the trajectories obtained in the present

study when performing cooling procedure. It was found that the molar volume decreases by about 15%, while the cohesive energy was increases by about 35%. Using these changes, solubility at room temperature turned out to be approximately 25% higher than at 550K, equaling to 18.0 ± 0.1 $(J/cm^3)^{0.5}$ for pure PLA and 17.6 ± 0.1 $(J/cm^3)^{0.5}$ for pure PHB. Thus, not only the decrease in volume, but also the increase in the cohesive energy results in the increase of the solubility parameter with temperature. It can be assumed that the decrease in volume results in shortening of interatomic distances and that, in turn, results in the increase of the cohesive energy between molecules and the total cohesive energy of the system. These new obtained solubility values are much closer to the ones in the experiments (19-20.5 $(J/cm^3)^{0.5}$ for PLA and 19.8 $(J/cm^3)^{0.5}$ for PHB) and in the HVK theory (20.8 $(J/cm^3)^{0.5}$ for PLA and 19.8 $(J/cm^3)^{0.5}$ for PHB) presented in Table 2.

The difference $\Delta\delta$ should be less than 2 $(J/cm^3)^{0.5}$ for two polymers to be miscible.[44] For pure PLA and PHB, this is satisfied by $\Delta\delta^{sim}$ as well as $\Delta\delta^{exp}$ and $\Delta\delta^{HVK}$, see Table 2. Thus, we can conclude that PLA and PHB should be miscible.

We estimated the χ values for all PLA and PHB blends studied (Table 2). The critical value of the Flory–Huggins parameter χ_{cr} for the chains of $N_p = 150$ monomers was equal to 0.013 (see details of the calculation in Supplementary Information). The results clearly indicate that the errors inherent in the direct calculation of the Flory–Huggins interaction parameters from the atomistic MD simulations using the internal energy change upon blending are too large to be useful for the prediction of miscibility. This contradicts the previous simulations which reported that MD method can be used to judge miscibility on the basis of the Flory–Huggins parameter.[32–41] The methodological result of this study is that the solubility parameter can be used for studying miscibility of polymers by atomistic MD simulations in system such as the current one.

We also tried to determine miscibility using the Flory-Huggins parameter by calculating it via change in the internal energy upon mixing[32,43] but were unable to obtain reliable results. In a very recent article, however, Zhang et al.[80] have introduced a new thermodynamic integration scheme that appears to allow for reliable determination of the χ-parameter from MD simulations. Such simulations are beyond the current work but the new scheme of Zhang et al. will be tested in future works and compared to using solubility.

Calculations of the glass transition temperature using the density change upon cooling. The transition of PLA-PHB blends from a melt to a glassy state has previously been investigated in a number of experimentals.[6,10,11,16,18,20] The pure PLA exhibits a glass transition around $T_g = 50$–$60°C$, while the pure PHB has $T_g = 4°C$, indicating that the difference in T_g between PLA and PHB is about 50 degrees.[1,2,20,31,81] It has been experimentally confirmed that the glass transition temperature of a blend decreases with increasing PHB fraction.[18,20] To verify the simulational approach, we compare the T_g values for the pure PLA and PHB, and the dependence of T_g on blend composition with experimental data. Moreover, using the cooling dependencies for the system density allows studies of the miscibility of PLA and PHB both in experiments[33,35–37] and simulations[10,11,17,18,20].

To compare with experiments, the cooling of PLA, PHB, and their blends has been simulated. We used the approach proposed in our previous studies of thermal properties of polymer systems.[45,59,62,63] For each system, 20 equilibrated configurations were stored every 200 ns. As follows from the results in Figure 3, during the time of 200 ns the monomers displace by a distance comparable to the corresponding R_g. In addition, 200 ns is an order of magnitude larger than the displacement time at distances of the order of the Kuhn segment of PLA and PHB.

Thus, we considered that the configurations separated by 200 ns should be more or less independent. The cooling of the systems from these selected configurations was simulated by a step-wise change in temperature: at each step, the temperature was decreased by 10 K, after that the system was simulated at this new temperature for 400 ps. Thus, the cooling rate was $2.5 \cdot 10^{10}$ K/s, which is usual for atomistic MD simulations.[45,59,62,63] For each of the studied systems, 20 temperature data points for the system density $\rho(T)$ were obtained, the averaged curves are shown in Figure 5a.
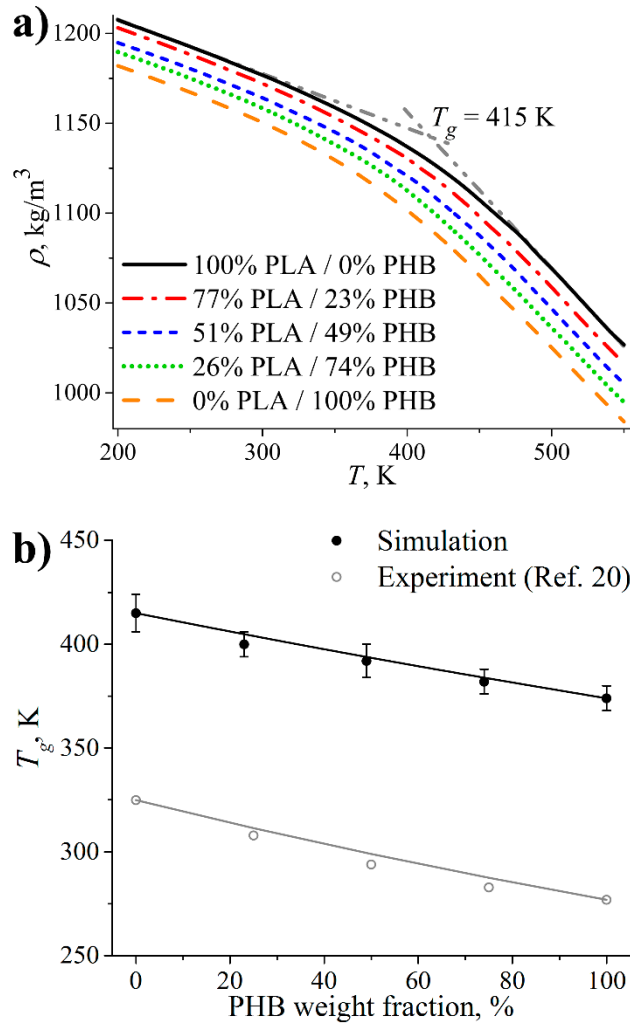

Figure 5. a) The dependence of system density ρ on temperature T. The dash-dot-dot lines illustrate the estimation of the glass transition temperatures for the pure PLA. b) The simulated

16

dependence of T_g on the PHB fraction in the blends (black) and the corresponding experimental curve[20] (gray). The lines are fits based on the Fox equation[82] $T_g^{Fox} = (\varphi_{PLA}/T_g^{PLA} + \varphi_{PHB}/T_g^{PHB})^{-1}$, where φ is a weight fraction of a certain polymer, decrease with increasing PHB fraction.

As seen from Figure 5a, all curves have linear regions with different slopes at the high and low temperatures. For each system, the T_g was determined from the intersection of the corresponding lines. Figure 5b shows that the values of T_g obtained from the simulations exceed significantly the experimental values of T_g. This is typical for atomistic simulations of polymers because the cooling rates used in simulations are more than 10 orders of magnitude higher than the experimental ones.[45,59,62,63] The simulated glass transition temperatures were estimated to be 415 ± 9 K and 374 ± 6 K for the pure PLA and PHB, respectively. Importantly, however, the simulated difference in the glass transition temperatures was 39 K, which agrees with the experimental data.[1,2,81,20,31] The values of T_g were calculated for the PLA-PHB blends as well. Figure 5b demonstrates that T_g decreases almost linearly with increasing PHB fraction. This agrees with experiments using blends of high molecular weight PHB ($M_w = 650$ kg/mol) with low molecular weight PLA ($M_w = 13$ kg/mol), see Figure 5b.[20] Moreover, the simulational and experimental curves in Figure 5b are parallel to each other, see fits of the curves using the Fox equation[82] $T_g^{Fox} = (\varphi_{PLA}/T_g^{PLA} + \varphi_{PHB}/T_g^{PHB})^{-1}$, where φ is a weight fraction of a certain polymer, decrease with increasing PHB fraction.

Summarizing the results above, we note that the analysis of the $\rho(T)$ dependence made it possible to obtain an excellent qualitative agreement with experiments; the simulations correctly reproduce the experimental difference in T_g for pure PLA and PHB, and the T_g dependence on

the PHB fraction in the blends. In addition, it was shown above that PLA is a more rigid polymer than PHB. Taken together, the results demonstrate the reliability of the model and methods.

Turning back to miscibility, note that in Figure 5a all the $\rho(T)$ curves have only one transition between the high and low temperature regimes. One transition is usually interpreted as evidence of miscibility, while two transitions imply immiscibility of polymers.[9,10,36] The fact that only one kink is observed in the $\rho(T)$ curves argues for miscibility of PLA and PHB chains. There is, however, a broad regime of transition temperatures. Namely, the width of the transition from the melt to the glassy state is of the order of 100 K, which exceeds the difference in the T_g values for PLA and PHB. Consequently, our analysis of $\rho(T)$ may not be conclusive enough to detect two glass transitions. Thus, we conclude that other methods should be used to fully clarify the miscibility of PLA and PHB.

Calculations of the glass transition temperature simulating the subchains mobility. Taking a step further, we utilized the MD data to extract the glass transition temperatures of the individual components of the blends. For this purpose, we adopted the method proposed by Doi et al.[83], and considered how the temperature change affects the mobility of PLA and PHB monomers. The mobility of the monomers was characterized by calculating their mean-square displacements and analysing them over a time interval of 400 ps vs. the inverse temperature $1/T$. At this time, the subdiffusive regime of the monomers was observed with the exponent of approximately 0.63 (see Supporting Information, Figure S1). Similar time interval was successfully used in Ref. 84 as well as in Ref. 85, where the very similar exponent of 0.66 was estimated. The results are shown in Figure 6 for both PLA (Figure 6a) and PHB (Figure 6b) monomers.
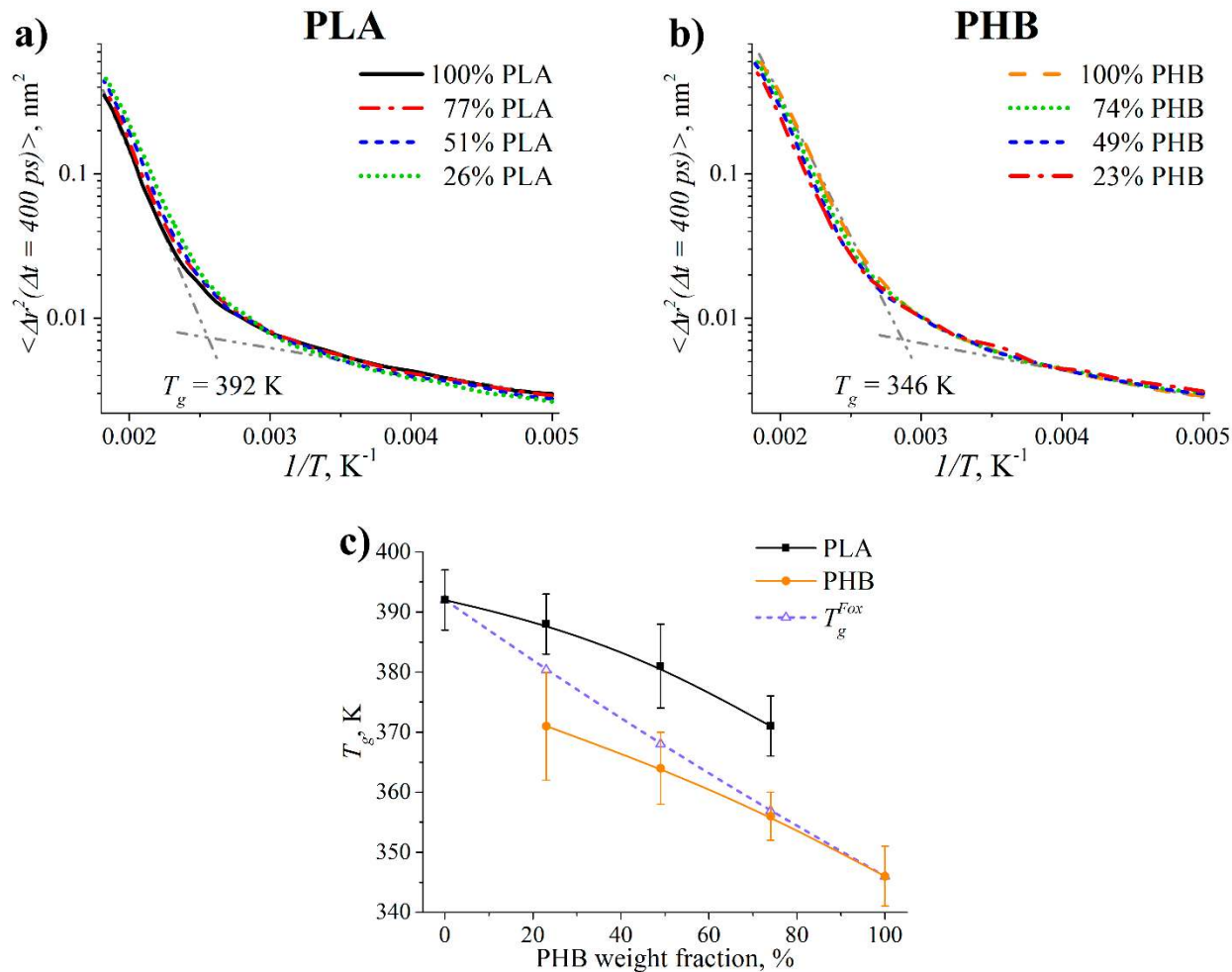
Figure 6. The semi-logarithmic plots of the mean-square displacements of monomers $\langle \Delta r^2 \rangle$ over 400 ps vs. the inverse temperature $1/T$ for the monomers of a) PLA and b) PHB. The dash-dot-dot lines are extrapolations to estimate T_g in pure PLA and PHB. The values of T_g for blends were determined the same way. c) Dependence of T_g on the PHB fraction in the blends calculated for the PLA (black) and PHB chains (orange). T_g^{Fox} is the glass transition temperature calculated according to the Fox equation[82] (violet). The lines are guides to the eye.

The temperature dependence of monomer mobility in the low- and high-temperature domains was approximated by linear functions; the T_g values were calculated as the intersection points,

see Figures 6a, b. In order to verify their correctness, we first compared the T_g values of pure PLA and PHB obtained from the Arrhenius curves $\langle \Delta r^2 \rangle (1/T)$ with those obtained earlier from the analysis of $\rho(T)$, see Figure 5. The values of T_g estimated dynamically were lower than those estimated from the density curves. The fact that the T_g values depend on the estimation method agrees with the results reported by Baljon et al.[86] Importantly, however, both approaches yield similar difference in T_g (about 40 K) between the pure PLA and PHB. In addition, the values of the mean glass transition temperature calculated with the Fox equation.[82] This behavior is similar to that presented in Figure 5b. Thus, the two methods for determining T_g give consistent results.

The fact that T_g decreases with increasing PHB fraction for both the PLA and PHB monomers indicates that their segmental mobilities strongly depend on their mutual interactions. The same conclusion can be drawn from Figure 3. This behavior would be impossible if they were immiscible. In a computational study[87] focusing on dynamic properties, clear differences between pure PEO and miscible blend of PEO/PMMA were observed consistently with the current simulations. However, the mean values of T_g^{PLA} and T_g^{PHB} differ by 15–20 K over the range of compositions and their error bars do not intersect. On the one hand, the presence of two T_g values in a polymer blend could be interpreted as an indicator of immiscibility.[9] On the other hand, the self-concentration model of Lodge and McLeish[12] states that two T_g values should be observed even in the case of the uniformly mixed blend. This stems from the hypothesis that at length scales of the order of the Kuhn segment, an essential part of the space around each monomer is occupied by the same monomers due to chain connectivity. The question arises: at

which length scales the two different T_g for PLA and PHB will become indistinguishable in the present simulations? To answer the question, we calculated the mean-square displacements of the centers of masses for the subchains of $N = 1$–30 neighboring monomers over 400 ps at different temperatures. From the temperature dependences of the displacements, we determined T_g for both the PLA and PHB subchains with different lengths N. In order to compare the data for PLA and PHB, we analyzed the dependence of the T_g using the mobility of the subchains with different end-to-end distance $H_{end-to-end}^{sub}$ which was calculated for the chosen values of N. The results are shown in Figure 7.
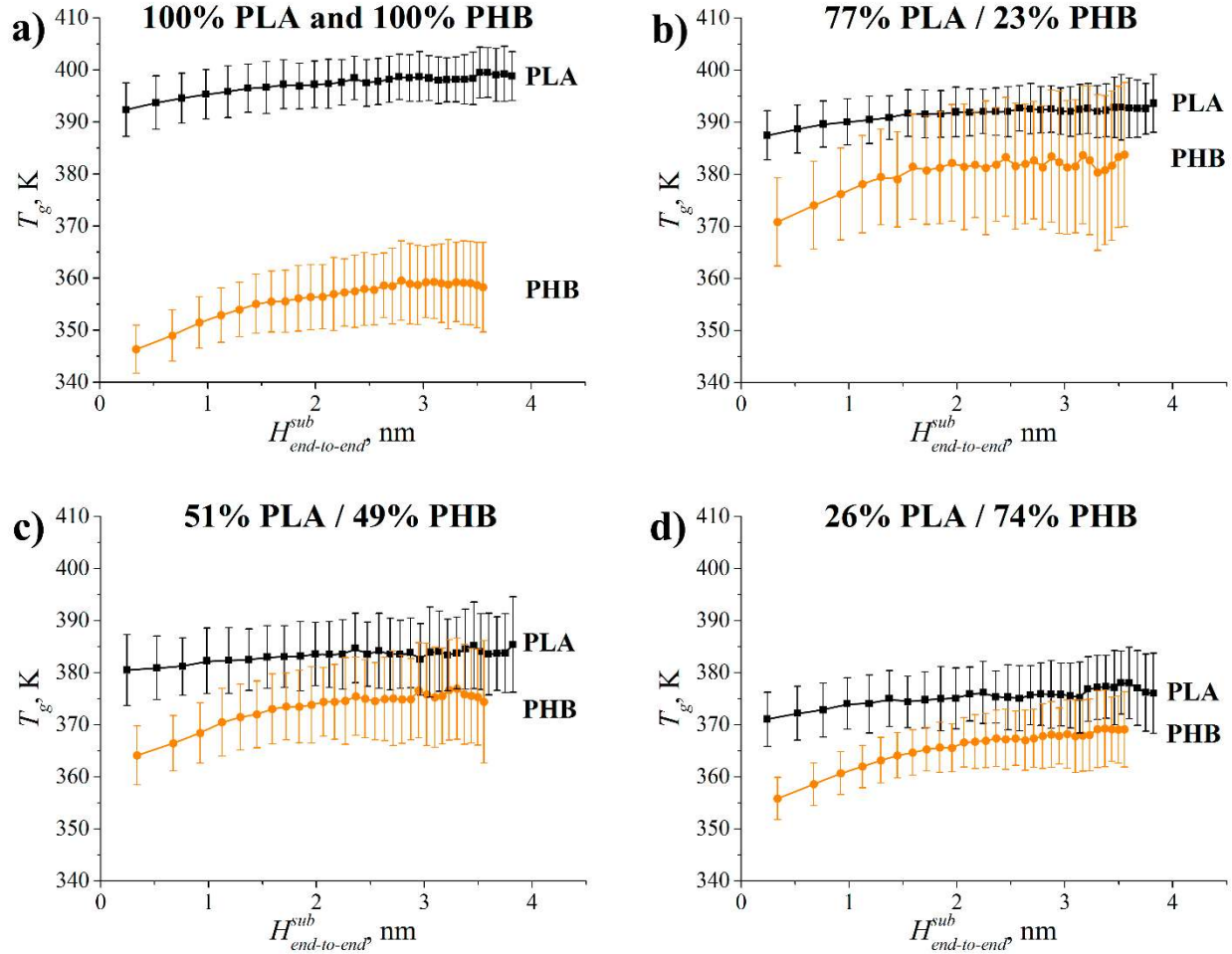
Figure 7. The dependence of T_g on the end-to-end distance $H^{sub}_{end-to-end}$ of subchains. The values of T_g were determined from the temperature dependence of the displacements of the centers of masses of subchains consisting of $N = 1$–30 neighboring monomers over 400 ps. Black lines: the data for PLA, orange: PHB. The PLA and PHB fractions are indicated inside the figures.

As Figure 7 shows, all curves grow rapidly for small subchains ($H^{sub}_{end-to-end} < 2$ nm). The growth then slows down and the dependencies saturate. For all systems considered, the initial increase of the T_g is steeper for PHB than for PLA. Regardless of the subchain size, the average values of T_g are higher for PLA than those for PHB. At the same time, an increase in the PHB

fraction results in a decrease of the T_g of PLA, and vice versa. A discrepancy between T_g for the pure PLA and PHB is about 40 K for all values of $H^{sub}_{end-to-end}$, see Figure 7a, while in the blends it is substantially smaller, see Figures 7c-d. As is evident from the Figures 7c-d, for small subchains with the size of 1–2 nm the corresponding error bars for T_g do not intersect, whereas at sizes larger than 1–2 nm the error bars start to intersect, i.e., the glass transition temperatures between PLA and PHB become indistinguishable within the margin of error. Therefore, we can conclude that PLA and PHB are semi-miscible at the length scale of 1–2 nm, while at the larger length scale they are miscible. The length scale of 1–2 nm corresponds to 1–2 Kuhn segments of PLA and PHB. This result is in line with the model of Lodge and McLeish where Kuhn segment is considered as a characteristic length scale of the self-concentration effect.[12]

Interaction of the components in the blends: interchain pair correlation functions. Lodge et al.[13] also suggested that the presence of two T_g cannot be used as a criterion of immiscibility and semi-miscibility. A local increase in the self-concentration due to chain connectivity of polymers is an intrachain effect.[12] Thus, the question arises whether different polymer chains are miscible on a length scale of several Kuhn segments. To address this question, we studied structural properties of the blends using the interchain pair correlation functions $g(r)$. These functions show the probability of finding atoms of chains of type A at a distance r from the atoms of the other chains of type B,[60]

$$g(r) = \frac{1}{4\pi r^2} \frac{1}{\rho_A \cdot N_B} \sum_{i \in B}^{N_B} \sum_{j \in A}^{N_A} \delta(r - r_{ij}), \qquad (2)$$

where ρ_A is the average number density of atoms in chains of type A, N_A and N_B are the numbers of atoms in chains of type A and B, respectively. r_{ij} is the distance between atoms in different chains of type A and B, and δ is the Dirac delta function.
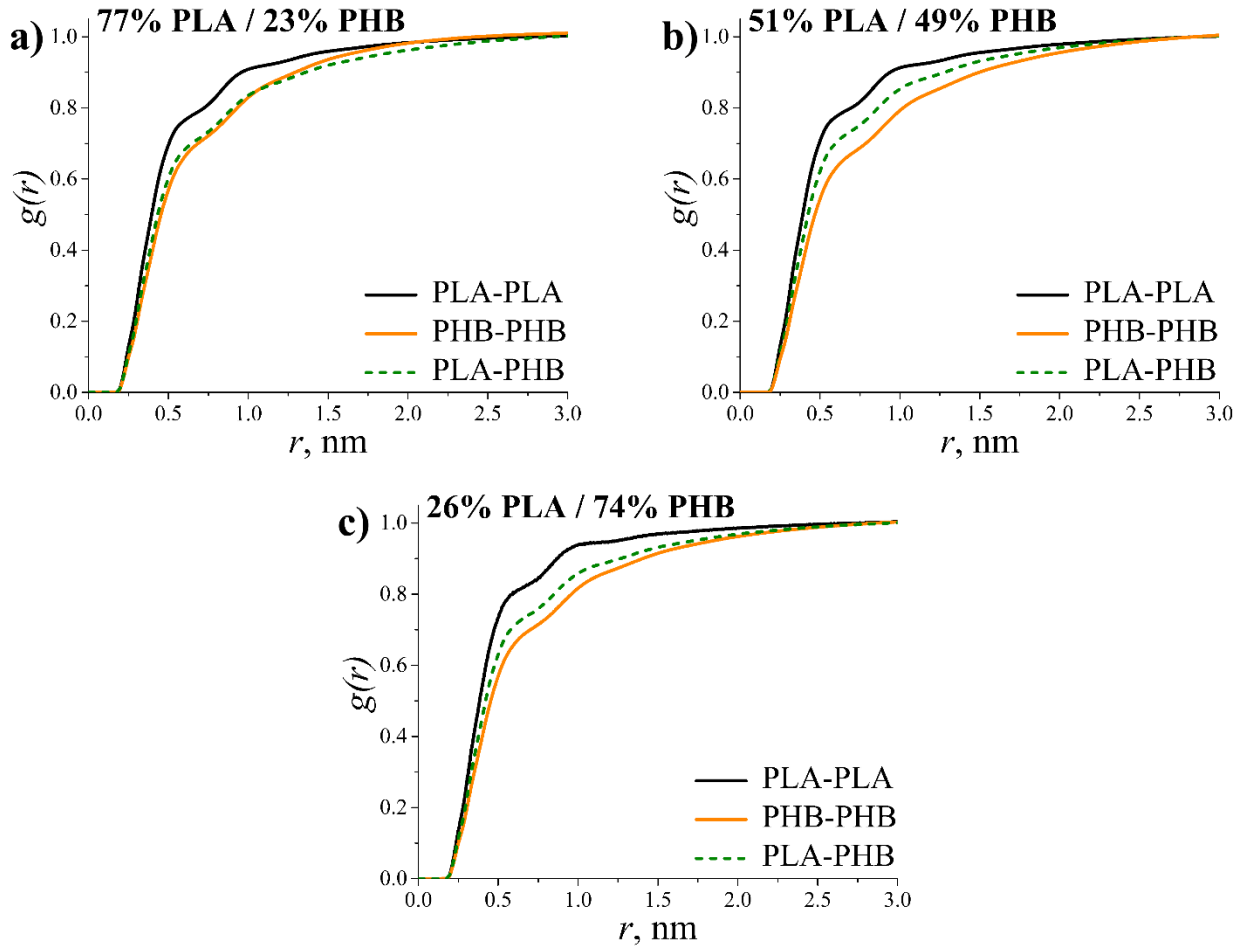

Figure 8. The interchain pair correlation functions between PLA-PLA (black solid lines), PHB-PHB (orange solid lines), and PLA-PHB (olive dashed lines) chains. The PLA and PHB fractions are indicated in the figures.

Figure 8 shows that in all blends the condition $g_{PHB-PHB}(r) \le g_{PLA-PHB}(r) \le g_{PLA-PLA}(r)$ is satisfied for $r < 2$ nm. This means that contacts between the PLA chains are the most probable, between the PLA and PHB chains less probable, and between the PHB chains the least probable. If PLA and PHB were completely miscible, the PLA-PHB curve would lie above both the PLA-PLA and PHB-PHB curves, while in the case of immiscibility the PLA-PHB curve would lie below both of them.[35] Thus, here we observe an intermediate case which means that within the length scale of 2 nm PLA and PHB are semi-miscible. It is important to notice that this intermolecular scale corresponds to the characteristic intrachain distance of 1–2 Kuhn segments where the values of T_g for PLA and PHB were distinct, as shown above in Figure 7. Thus, this confirms that PLA and PHB are semi-miscible in the scale of Kuhn segments. Concerning the distances exceeding 1–2 Kuhn segments, Figure 8 shows that the difference between PLA-PLA, PHB-PHB, and PLA-PHB curves becomes small. Thus, we conclude that at this length scale PLA and PHB are miscible. This also implies that miscibility of PLA and PHB is scale-dependent. We would like to point out, however, that in the cases of 23% PHB and 26% PLA, the number of minority component chains is small (although the number of monomers per chain is reasonably large, Table 1).

It is worth mentioning the influence of the finite-size effects in the present simulations. Figure 8 shows that the systems sizes are large enough, and the finite-size effects are small, since all the curves approach unity.[88,89] To corroborate this conclusion further we performed additional simulations of a larger system (with the PHB weight fraction of 49%) composed of 18 PHB chains and 22 PLA chains. The simulations run for 200 ns at a pressure of 1 bar and a temperature of 550 K. The interchain pair correlation functions between the components of this system, averaged over the last 20 ns of the trajectory, are shown below, see Figure 9.
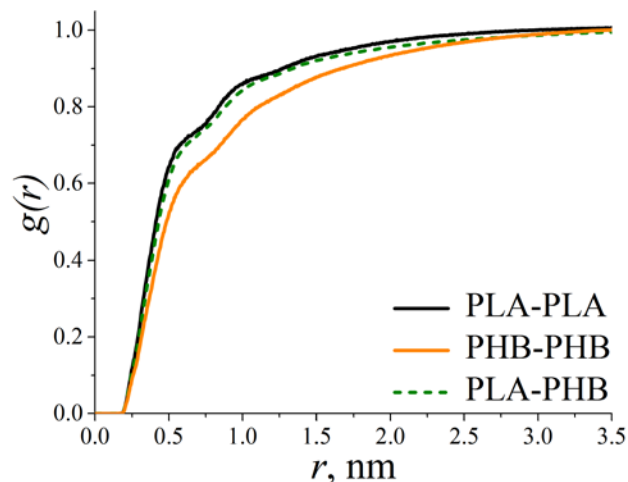
Figure 9. The interchain pair correlation functions between PLA-PLA (black solid lines), PHB-PHB (orange solid lines), and PLA-PHB (olive dashed lines) chains in the blend composed of 18 PHB chains and 22 PLA chains, with PHB weight fraction of 49%. .

As seen from the Figure 9, there is a small quantitative difference of the results within the distances of about 2 nm, compared to those for the twice smaller system, see Figure 8b. Namely, the PLA-PHB curve lies close to the PLA-PLA curve in the former case, whereas the same curve lies between PLA-PLA and PHB-PHB in the latter case. The obtained small difference can be attributed to the shorter simulation times of the performed test run. Thus, these additional simulations show that the finite-size effects do not significantly influence the results for the systems considered in the present study.

The obtained miscibility of PLA and PHB at length scales exceeding the Kuhn segment can be considered in the context of the previous findings of White and Lipson.[90] They noted that the smaller the difference between the energies of nonbonded segment−segment interactions of pure components, the greater the tendency of the blended components towards miscibility. Due to high chemical similarity of PLA and PHB, this difference is likely to be small. Therefore, miscibility between components can be observed.

Our results are in line with the experiments of Se et al.[91] They used blends of miscible polystyrene (PS) and polyisoprene (PI) and concluded that the blend is homogeneous at the length scales of polymer chain sizes and is weakly segregated at the monomer scale. Faller et al.[92] observed a slight structural inhomogeneity at a monomer scale in their atomistic simulations of PS-PI blends. They noted that it was not possible to study phase separation of polymer chains due to rather short (~2 ns) simulation times. Our MD trajectories are three orders of magnitude longer (μs vs ns) and show that local inhomogeneity in blends does not lead to phase separation. Finally, the current results are in line with the comprehensive study of PI/PS blends reported by Harmandaris et al.[93] Using calculations of the distance dependence of self- and effective concentrations for the chains, they showed that both intra- and intermolecular local environments of the blend component at the length scales of the Kuhn segments differ from the ones at larger length scales.

IV. CONCLUSIONS

Miscibility of PLA and PHB was studied by atomistic MD simulations. Five systems with PHB weight fractions between 0 to 100% were considered. The molecular weights of the PLA and PHB chains were chosen to be relatively small (about 10 kg/mol), since miscibility for such chains is expected. The Flory–Huggins theory was used to calculate the solubility (δ) and interaction parameters (χ) for the blends of PLA and PHB. It was shown that the difference in the PLA and PHB solubility parameters is less than 2 $(J/cm^3)^{0.5}$ which argues for their miscibility. As for the Flory–Huggins parameter χ, we have shown that it cannot be used as a reliable criterion of miscibility in MD simulations due to rather high statistical fluctuations.

Miscibility of PLA and PHB was also studied using the temperature dependence of system density, $\rho(T)$. It was shown that in all systems the $\rho(T)$ curves display only one kink corresponding to the transition to a glassy state. However, this cannot be considered as a reliable indicator of miscibility, since the width of transition region was too large to distinguish two kinks. For this reason, we divided the PLA and PHB chains into subchains of neighboring monomers and studied the dependence of T_g on subchain size by analyzing the mobility of the subchains. It turned out that the values of T_g for PLA and PHB were indistinguishable within the margin of error at the length scale of 1–2 nm, which corresponds to 1–2 Kuhn segments of PLA and PHB. For shorter subchains, two distinct T_g values were found for PLA and PHB in the blends over the entire range of composition. The presence of two T_g values in blends is in line with the self-concentration model of Lodge and McLeish: within a sphere of the size of the Kuhn segment, the concentration of a polymer is increased due to chain connectivity, and thus two T_g values are expected even for miscible polymers.

In order to check whether PLA and PHB are miscible within 2 nm, we also analyzed the interchain pair correlation functions. It was found that at this length scale they are semi-miscible. The obtained results allowed us to conclude that the structural properties of polymer blends may be scale-dependent: they may differ at the Kuhn segment scale from those at larger length scales. Both inter- and intrachain structural heterogeneity were found to be important for studying the segmental dynamics in blends of miscible polymers.[94–97] The observed miscibility of low molecular weight PLA and PHB in length scales exceeding the Kuhn segment enables us to assume that the criteria of miscibility investigated in the present study should be helpful in resolving the important question of miscibility in other systems.

ASSOCIATED CONTENT

Supporting Information

Calculation of characteristic equilibration time, verification of the equilibrium states and model validation, calculation of solubility parameters δ and Flory–Huggins interaction parameters χ, estimate for diffusive regime. The force field parameters as well as atomic coordinate files for PLA and PHB chains used in the present study.

AUTHOR INFORMATION

Corresponding Author

*E-mail s.v.lyulin@gmail.com (S.V.L.).

Author Contributions

The manuscript was written through contributions of all authors. All authors have given approval to the final version of the manuscript. All authors contributed equally.

ACKNOWLEDGMENTS

REFERENCES

(1) Auras, R.; Harte, B.; Selke, S. An Overview of Polylactides as Packaging Materials. *Macromol. Biosci.* **2004**, *4* (9), 835–864 DOI: 10.1002/mabi.200400043.

(2) Sudesh, K.; Abe, H.; Doi, Y. Synthesis, Structure and Properties of Polyhydroxyalkanoates: Biological Polyesters. *Prog. Polym. Sci.* **2000**, *25* (10), 1503–1555 DOI: 10.1016/S0079-6700(00)00035-6.

(3) Gironi, F.; Piemonte, V. Bioplastics and Petroleum-Based Plastics: Strengths and Weaknesses. *Energy Sources, Part A Recover. Util. Environ. Eff.* **2011**, *33* (21), 1949–1959 DOI: 10.1080/15567030903436830.

(4) Arrieta, M.; Samper, M.; Aldas, M.; López, J. On the Use of PLA-PHB Blends for Sustainable Food Packaging Applications. Materials. 2017, 10 (9), 1008 DOI: 10.3390/ma10091008.

(5) S. de O. Patrício, P.; Pereira, F. V.; dos Santos, M. C.; de Souza, P. P.; Roa, J. P. B.; Orefice, R. L. Increasing the Elongation at Break of Polyhydroxybutyrate Biopolymer: Effect of Cellulose Nanowhiskers on Mechanical and Thermal Properties. J. Appl. Polym. Sci. 2013, 127 (5), 3613–3621 DOI: 10.1002/app.37811.

(6) Zhang, M.; Thomas, N. L. Blending Polylactic Acid with Polyhydroxybutyrate: The Effect on Thermal, Mechanical, and Biodegradation Properties. Adv. Polym. Technol. 2011, 30 (2), 67–79 DOI: 10.1002/adv.20235.

(7) Lai, S.-M.; Liu, Y.-H.; Huang, C.-T.; Don, T.-M. Miscibility and Toughness Improvement of Poly(lactic acid)/poly(3-Hydroxybutyrate) Blends Using a Melt-Induced Degradation Approach. J. Polym. Res. 2017, 24 (7), 102 DOI: 10.1007/s10965-017-1253-0.

(8)   Park, J. W.; Doi, Y.; Iwata, T. Uniaxial Drawing and Mechanical Properties of Poly[(R)-3-hydroxybutyrate]/Poly(L-lactic acid) Blends. *Biomacromolecules* **2004**, *5* (4), 1557–1566 DOI: 10.1021/bm049905l.

(9)   Thomas, S.; Grohens, Y.; Jyotishkumar, P. *Characterization of Polymer Blends: Miscibility, Morphology and Interfaces*; Thomas, S., Grohens, Y., Jyotishkumar, P., Eds.; Wiley-VCH Verlag: Weinheim, Germany, 2014.

(10) Kikkawa, Y.; Suzuki, T.; Kanesato, M.; Doi, Y.; Abe, H. Effect of Phase Structure on Enzymatic Degradation in Poly(L-lactide)/Atactic Poly(3-hydroxybutyrate) Blends with Different Miscibility. *Biomacromolecules* **2009**, *10* (4), 1013–1018 DOI: 10.1021/bm900117j.

(11) Arias, V.; Höglund, A.; Odelius, K.; Albertsson, A.-C. Tuning the Degradation Profiles of Poly(L-lactide)-Based Materials through Miscibility. *Biomacromolecules* **2014**, *15* (1), 391–402 DOI: 10.1021/bm401667b.

(12) Lodge, T. P.; McLeish, T. C. B. Self-Concentrations and Effective Glass Transition Temperatures in Polymer Blends. *Macromolecules* **2000**, *33* (14), 5278–5284 DOI: 10.1021/ma9921706.

(13) Lodge, T. P.; Wood, E. R.; Haley, J. C. Two Calorimetric Glass Transitions Do Not Necessarily Indicate Immiscibility: The Case of PEO/PMMA. *J. Polym. Sci. Part B Polym. Phys.* **2006**, *44* (4), 756–763 DOI: 10.1002/polb.20735.

(14) He, Y.; Lutz, T. R.; Ediger, M. D. Segmental and Terminal Dynamics in Miscible Polymer Mixtures: Tests of the Lodge–McLeish Model. *J. Chem. Phys.* **2003**, *119* (18), 9956–9965 DOI: 10.1063/1.1615963.

(15) Qiu, J.; Xing, C.; Cao, X.; Wang, H.; Wang, L.; Zhao, L.; Li, Y. Miscibility and Double Glass Transition Temperature Depression of Poly(L-lactic acid) (PLLA)/Poly(oxymethylene) (POM) Blends. *Macromolecules* **2013**, *46* (14), 5806–5814 DOI: 10.1021/ma401084y.

(16) Arrieta, M. P.; Samper, M. D.; López, J.; Jiménez, A. Combined Effect of Poly(hydroxybutyrate) and Plasticizers on Polylactic Acid Properties for Film Intended for Food Packaging. *J. Polym. Environ.* **2014**, *22* (4), 460–470 DOI: 10.1007/s10924-014-0654-y.

(17) Focarete, M. L.; Ceccorulli, G.; Scandola, M.; Kowalczuk, M. Further Evidence of Crystallinity-Induced Biodegradation of Synthetic Atactic Poly(3-hydroxybutyrate) by PHB-Depolymerase A from Pseudomonas L Emoignei . Blends of Atactic Poly(3-hydroxybutyrate) with Crystalline Polyesters. *Macromolecules* **1998**, *31* (24), 8485–8492 DOI: 10.1021/ma981115e.

(18) Ohkoshi, I.; Abe, H.; Doi, Y. Miscibility and Solid-State Structures for Blends of poly[(S)-lactide] with Atactic poly[(R,S)-3-hydroxybutyrate]. *Polymer* **2000**, *41* (15), 5985–5992 DOI: 10.1016/S0032-3861(99)00781-8.

(19) Gazzano, M.; Focarete, M. L.; Riekel, C.; Scandola, M. Structural Study of Poly(L-lactic acid) Spherulites. *Biomacromolecules* **2004**, *5* (2), 553–558 DOI: 10.1021/bm0343951.

(20) Koyama, N.; Doi, Y. Miscibility of Binary Blends of poly[(R)-3-hydroxybutyric acid] and poly[(S)-lactic acid]. *Polymer* **1997**, *38* (7), 1589–1593 DOI: 10.1016/S0032-3861(96)00685-4.

(21) Blümm, E.; Owen, A. J. Miscibility, Crystallization and Melting of poly(3-hydroxybutyrate)/poly(L-lactide) Blends. *Polymer* **1995**, *36* (21), 4077–4081 DOI: 10.1016/0032-3861(95)90987-D.

(22) Yoon, J.-S.; Lee, W.-S.; Kim, K.-S.; Chin, I.-J.; Kim, M.-N.; Kim, C. Effect of Poly(ethylene glycol)-Block-poly(L-lactide) on the poly[(R)-3-hydroxybutyrate]/poly(L-lactide) Blends. *Eur. Polym. J.* **2000**, *36* (2), 435–442 DOI: 10.1016/S0014-3057(99)00068-3.

(23) Sun, X.; Tokuda, A.; Oji, Y.; Nakatani, T.; Tsuji, H.; Ozaki, Y.; Yan, S.; Takahashi, I. Effects of Molar Mass of Poly(L-lactide acid) on the Crystallization of Poly[(R)-3-hydroxybutyrate] in Their Ultrathin Blend Films. *Macromolecules* **2012**, *45* (5), 2485–2493 DOI: 10.1021/ma202543s.

(24) Zhang, L.; Xiong, C.; Deng, X. Miscibility, Crystallization and Morphology of Poly(β-hydroxybutyrate)/poly(D,L-lactide) Blends. *Polymer* **1996**, *37* (2), 235–241 DOI: 10.1016/0032-3861(96)81093-7.

(25) Vogel, C.; Wessel, E.; Siesler, H. W. FT-IR Imaging Spectroscopy of Phase Separation in Blends of Poly(3-hydroxybutyrate) with Poly(L-lactic acid) and Poly(ε-caprolactone). *Biomacromolecules* **2008**, *9* (2), 523–527 DOI: 10.1021/bm701035p.

(26) Vogel, C.; Wessel, E.; Siesler, H. W. FT-IR Spectroscopic Imaging of Anisotropic Poly(3-hydroxybutyrate)/Poly(lactic acid) Blends with Polarized Radiation. *Macromolecules* **2008**, *41* (9), 2975–2977 DOI: 10.1021/ma800139u.

(27) Zhang, J.; Sato, H.; Furukawa, T.; Tsuji, H.; Noda, I.; Ozaki, Y. Crystallization Behaviors of Poly(3-hydroxybutyrate) and Poly(L-lactic acid) in Their Immiscible and Miscible Blends. *J. Phys. Chem. B* **2006**, *110* (48), 24463–24471 DOI: 10.1021/jp065233c.

(28) D'Amico, D. A.; Iglesias Montes, M. L.; Manfredi, L. B.; Cyras, V. P. Fully Bio-Based and Biodegradable Polylactic acid/poly(3-hydroxybutirate) Blends: Use of a Common Plasticizer as Performance Improvement Strategy. *Polym. Test.* **2016**, *49*, 22–28 DOI: 10.1016/j.polymertesting.2015.11.004.

(29) Furukawa, T.; Sato, H.; Murakami, R.; Zhang, J.; Duan, Y. X.; Noda, I.; Ochiai, S.; Ozaki, Y. Structure, Dispersibility, and Crystallinity of Poly(hydroxybutyrate)/ poly(L-lactic acid) Blends Studied by FT-IR Microspectroscopy and Differential Scanning Calorimetry. *Macromolecules* **2005**, *38* (15), 6445–6454 DOI: 10.1021/ma0504668.

(30) Furukawa, T.; Sato, H.; Murakami, R.; Zhang, J.; Noda, I.; Ochiai, S.; Ozaki, Y. Raman Microspectroscopy Study of Structure, Dispersibility, and Crystallinity of Poly(hydroxybutyrate)/poly(L-lactic acid) Blends. *Polymer* **2006**, *47* (9), 3132–3140 DOI: 10.1016/j.polymer.2006.03.010.

(31) Furukawa, T.; Sato, H.; Murakami, R.; Zhang, J.; Noda, I.; Ochiai, S.; Ozaki, Y. Comparison of Miscibility and Structure of poly(3-hydroxybutyrate-co-3-hydroxyhexanoate)/poly(L-lactic acid) Blends with Those of poly(3-hydroxybutyrate)/poly(L-lactic acid) Blends Studied by Wide Angle X-Ray Diffraction, Differential Scanning Calorimetry. *Polymer* **2007**, *48* (6), 1749–1755 DOI: 10.1016/j.polymer.2007.01.020.

(32) Martinez de Arenaza, I.; Hernandez-Montero, N.; Meaurio, E.; Sarasua, J.-R. Competing Specific Interactions Investigated by Molecular Dynamics: Analysis of Poly(p-

dioxanone)/Poly(vinyl phenol) Blends. *J. Phys. Chem. B* **2012**, *117* (2), 719–724 DOI: 10.1021/jp310340v.

(33) Gupta, J.; Nunes, C.; Vyas, S.; Jonnalagadda, S. Prediction of Solubility Parameters and Miscibility of Pharmaceutical Compounds by Molecular Dynamics Simulations. *J. Phys. Chem. B* **2011**, *115* (9), 2014–2023 DOI: 10.1021/jp108540n.

(34) Jawalkar, S. S.; Aminabhavi, T. M. Molecular Modeling Simulations and Thermodynamic Approaches to Investigate Compatibility/incompatibility of poly(L-lactide) and Poly(vinyl alcohol) Blends. *Polymer* **2006**, *47* (23), 8061–8071 DOI: 10.1016/j.polymer.2006.09.030.

(35) Luo, Z.; Jiang, J. Molecular Dynamics and Dissipative Particle Dynamics Simulations for the Miscibility of Poly(ethylene oxide)/poly(vinyl chloride) Blends. *Polymer* **2010**, *51* (1), 291–299 DOI: 10.1016/j.polymer.2009.11.024.

(36) Saha, S.; Bhowmick, A. K. Computer Simulation of Thermoplastic Elastomers from Rubber-Plastic Blends and Comparison with Experiments. *Polymer* **2016**, *103*, 233–242 DOI: 10.1016/j.polymer.2016.09.065.

(37) Yang, H.; Li, Z.-S.; Lu, Z.-Y.; Sun, C.-C. Computer Simulation Studies of the Miscibility of poly(3-hydroxybutyrate)-Based Blends. *Eur. Polym. J.* **2005**, *41* (12), 2956–2962 DOI: 10.1016/j.eurpolymj.2005.06.009.

(38) Xu, Y.; Koo, D.; Gerstein, E. A.; Kim, C.-S. Multi-Scale Modeling of Polymer-Drug Interactions and Their Impact on the Structural Evolutions in PLGA-Tetracycline Films. *Polymer* **2016**, *84*, 121–131 DOI: 10.1016/j.polymer.2015.12.052.

(39) Wei, Q.; Wang, Y.; Che, Y.; Yang, M.; Li, X.; Zhang, Y. Molecular Mechanisms in Compatibility and Mechanical Properties of Polyacrylamide/Polyvinyl Alcohol Blends. *J. Mech. Behav. Biomed. Mater.* **2017**, *65*, 565–573 DOI: 10.1016/j.jmbbm.2016.09.011.

(40) Erlebach, A.; Ott, T.; Otzen, C.; Schubert, S.; Czaplewska, J.; Schubert, U. S.; Sierka, M. Thermodynamic Compatibility of Actives Encapsulated into PEG-PLA Nanoparticles: In Silico Predictions and Experimental Verification. *J. Comput. Chem.* **2016**, *37* (24), 2220–2227 DOI: 10.1002/jcc.24449.

(41) Spyriouni, T.; Vergelati, C. A Molecular Modeling Study of Binary Blend Compatibility of Polyamide 6 and Poly(vinyl acetate) with Different Degrees of Hydrolysis: An Atomistic and Mesoscopic Approach. *Macromolecules* **2001**, *34* (15), 5306–5316 DOI: 10.1021/ma001669t.

(42) May, A. F.; Maranas, J. K. The Single Chain Limit of Structural Relaxation in a Polyolefin Blend. *J. Chem. Phys.* **2006**, *125* (2), 24906 DOI: 10.1063/1.2204034.

(43) Patel, S.; Lavasanifar, A.; Choi, P. Application of Molecular Dynamics Simulation To Predict the Compatability between Water-Insoluble Drugs and Self-Associating Poly(ethylene oxide)-*b*-Poly(ε-caprolactone) Block Copolymers. *Biomacromolecules* **2008**, *9* (11), 3014–3023 DOI: 10.1021/bm800320z.

(44) Coleman, M. M.; Serman, C. J.; Bhagwagar, D. E.; Painter, P. C. A Practical Guide to Polymer Miscibility. *Polymer* **1990**, *31* (7), 1187–1203 DOI: 10.1016/0032-3861(90)90208-G.

(45) Lyulin, S. V.; Gurtovenko, A. A.; Larin, S. V.; Nazarychev, V. M.; Lyulin, A. V. Microsecond Atomic-Scale Molecular Dynamics Simulations of Polyimides. *Macromolecules* **2013**, *46* (15), 6357–6363 DOI: 10.1021/ma4011632.

(46) Jamshidi, K.; Hyon, S. H.; Ikada, Y. Thermal Characterization of Polylactides. *Polymer* **1988**, *29* (12), 2229–2234 DOI: 10.1016/0032-3861(88)90116-4.

(47) Wang, J. M.; Wolf, R. M.; Caldwell, J. W.; Kollman, P. A.; Case, D. A. Development and Testing of a General Amber Force Field. *J. Comput. Chem.* **2004**, *25* (9), 1157–1174 DOI: 10.1002/jcc.20035.

(48) Lin, P.-H.; Khare, R. Molecular Simulation of Cross-Linked Epoxy and Epoxy−POSS Nanocomposite. *Macromolecules* **2009**, *42* (12), 4319–4327 DOI: 10.1021/ma9004007.

(49) Khabaz, F.; Mani, S.; Khare, R. Molecular Origins of Dynamic Coupling between Water and Hydrated Polyacrylate Gels. *Macromolecules* **2016**, *49* (19), 7551–7562 DOI: 10.1021/acs.macromol.6b00938.

(50) Sprenger, K. G.; Jaeger, V. W.; Pfaendtner, J. The General AMBER Force Field (GAFF) Can Accurately Predict Thermodynamic and Transport Properties of Many Ionic Liquids. *J. Phys. Chem. B* **2015**, *119* (18), 5882–5895 DOI: 10.1021/acs.jpcb.5b00689.

(51) Spahn, V.; Del Vecchio, G.; Labuz, D.; Rodriguez-Gaztelumendi, A.; Massaly, N.; Temp, J.; Durmaz, V.; Sabri, P.; Reidelbach, M.; Machelska, H.; Weber, M.; Stein, C. A Nontoxic Pain Killer Designed by Modeling of Pathological Receptor Conformations. *Science* **2017**, *355* (6328), 966–969 DOI: 10.1126/science.aai8636.

(52) Khare, K. S.; Khabaz, F.; Khare, R. Effect of Carbon Nanotube Functionalization on Mechanical and Thermal Properties of Cross-Linked Epoxy–Carbon Nanotube Nanocomposites: Role of Strengthening the Interfacial Interactions. *ACS Appl. Mater. Interfaces* **2014**, *6* (9), 6098–6110 DOI: 10.1021/am405317x.

(53) Wong-ekkabut, J.; Karttunen, M. The Good, the Bad and the User in Soft Matter Simulations. Biochim. Biophys. Acta - Biomembr. 2016, 1858 (10), 2529–2538 DOI: 10.1016/j.bbamem.2016.02.004.

(54) Sousa da Silva, A. W.; Vranken, W. F. ACPYPE - AnteChamber PYthon Parser interfacE. *BMC Res. Notes* **2012**, *5* (1), 367 DOI: 10.1186/1756-0500-5-367.

(55) Wang, J.; Wang, W.; Kollman, P. A.; Case, D. A. Automatic Atom Type and Bond Type Perception in Molecular Mechanical Calculations. *J. Mol. Graph. Model.* **2006**, *25* (2), 247–260 DOI: 10.1016/j.jmgm.2005.12.005.

(56) Frisch, M. J.; Trucks, G. W.; Schlegel, H. B.; Scuseria, G. E.; Robb, M. A.; Cheeseman, J. R.; Scalmani, G.; Barone, V.; Mennucci, B.; Petersson, G. A.; Nakatsuji, H.; Caricato, M.; Li, X.; Hratchian, H. P.; Izmaylov, A. F.; Bloino, J.; Zheng, G.; Sonnenberg, J. L.; Hada, M.; Ehara, M.; Toyota, K.; Fukuda, R.; Hasegawa, J.; Ishida, M.; Nakajima, T.; Honda, Y.; Kitao, O.; Nakai, H.; Vreven, T.; Montgomery, J. A.; Peralta, J. E.; Ogliaro, F.; Bearpark, M.; Heyd, J. J.; Brothers, E.; Kudin, K. N.; Staroverov, V. N.; Kobayashi, R.; Normand, J.; Raghavachari, K.; Rendell, A.; Burant, J. C.; Iyengar, S. S.; Tomasi, J.; Cossi, M.; Rega, N.; Millam, J. M.; Klene, M.; Knox, J. E.; Cross, J. B.; Bakken, V.; Adamo, C.; Jaramillo, J.; Gomperts, R.; Stratmann, R. E.; Yazyev, O.; Austin, A. J.; Cammi, R.; Pomelli, C.; Ochterski, J. W.; Martin, R. L.; Morokuma, K.; Zakrzewski, V. G.; Voth, G. A.; Salvador, P.; Dannenberg, J. J.; Dapprich, S.; Daniels, A. D.; Farkas, Ö.; Foresman, J. B.; Ortiz, J. V.; Cioslowski, J.; Fox, D. J. Gaussian 09, Gaussian, Inc. Wallingford CT 2009.

(57) Lukasheva, N. V.; Tolmachev, D. A.; Nazarychev, V. M.; Kenny, J. M.; Lyulin, S. V. Influence of Specific Intermolecular Interactions on the Thermal and Dielectric Properties of

Bulk Polymers: Atomistic Molecular Dynamics Simulations of Nylon 6. *Soft Matter* **2017**, *13* (2), 474–485 DOI: 10.1039/C6SM02169G.

(58) Borzdun, N. I.; Larin, S. V.; Falkovich, S. G.; Nazarychev, V. M.; Volgin, I. V.; Yakimansky, A. V.; Lyulin, A. V.; Negi, V.; Bobbert, P. A.; Lyulin, S. V. Molecular Dynamics Simulation of poly(3-hexylthiophene) Helical Structure In Vacuo and in Amorphous Polymer Surrounding. *J. Polym. Sci. Part B Polym. Phys.* **2016**, *54* (23), 2448–2456 DOI: 10.1002/polb.24236.

(59) Lyulin, S. V; Larin, S. V; Gurtovenko, A. A.; Nazarychev, V. M.; Falkovich, S. G.; Yudin, V. E.; Svetlichnyi, V. M.; Gofman, I. V; Lyulin, A. V. Thermal Properties of Bulk Polyimides: Insights from Computer Modeling versus Experiment. *Soft Matter* **2014**, *10* (8), 1224–1232 DOI: 10.1039/c3sm52521j.

(60) Larin, S. V.; Falkovich, S. G.; Nazarychev, V. M.; Gurtovenko, A. A.; Lyulin, A. V.; Lyulin, S. V. Molecular-Dynamics Simulation of Polyimide Matrix Pre-Crystallization near the Surface of a Single-Walled Carbon Nanotube. *RSC Adv.* **2014**, *4* (2), 830–844 DOI: 10.1039/C3RA45010D.

(61) Larin, S. V.; Glova, A. D.; Serebryakov, E. B.; Nazarychev, V. M.; Kenny, J. M.; Lyulin, S. V. Influence of the Carbon Nanotube Surface Modification on the Microstructure of Thermoplastic Binders. *RSC Adv.* **2015**, *5* (64), 51621–51630 DOI: 10.1039/C5RA07851B.

(62) Nazarychev, V. M.; Larin, S. V.; Yakimansky, A. V.; Lukasheva, N. V.; Gurtovenko, A. A.; Gofman, I. V.; Yudin, V. E.; Svetlichnyi, V. M.; Kenny, J. M.; Lyulin, S. V. Parameterization of Electrostatic Interactions for Molecular Dynamics Simulations of

Heterocyclic Polymers. *J. Polym. Sci. Part B Polym. Phys.* **2015**, *53* (13), 912–923 DOI: 10.1002/polb.23715.

(63) Glova, A. D.; Falkovich, S. G.; Larin, S. V; Mezhenskaia, D. A.; Lukasheva, N. V; Nazarychev, V. M.; Tolmachev, D. A.; Mercurieva, A. A.; Kenny, J. M.; Lyulin, S. V. Poly(lactic acid)-Based Nanocomposites Filled with Cellulose Nanocrystals with Modified Surface: All-Atom Molecular Dynamics Simulations. *Polym. Int.* **2016**, *65* (8), 892–898 DOI: 10.1002/pi.5102.

(64) Falkovich, S. G.; Larin, S. V.; Lukasheva, N. V.; Nazarychev, V. M.; Tolmachev, D. A.; Glova, A. D.; Mezhenskaia, D. A.; Kenny, J. M.; Lyulin, S. V. Computational Modeling of Polylactide and Its Cellulose-Reinforced Nanocomposites. In *Multifunctional Polymeric Nanocomposites Based on Cellulosic Reinforcements*; Elsevier, 2016; pp 313–341.

(65) Nazarychev, V. M.; Lyulin, A. V.; Larin, S. V.; Gofman, I. V.; Kenny, J. M.; Lyulin, S. V. Correlation between the High-Temperature Local Mobility of Heterocyclic Polyimides and Their Mechanical Properties. *Macromolecules* **2016**, *49* (17), 6700–6710 DOI: 10.1021/acs.macromol.6b00602.

(66) Volgin, I. V.; Larin, S. V.; Abad, E.; Lyulin, S. V. Molecular Dynamics Simulations of Fullerene Diffusion in Polymer Melts. *Macromolecules* **2017**, *50* (5), 2207–2218 DOI: 10.1021/acs.macromol.6b02050.

(67) Lyulin, S. V; Larin, S. V; Nazarychev, V. M.; Fal'kovich, S. G.; Kenny, J. M. Multiscale Computer Simulation of Polymer Nanocomposites Based on Thermoplastics. *Polym. Sci. Ser. C* **2016**, *58* (1), 2–15 DOI: 10.1134/S1811238216010082.

(68) Nazarychev, V. M.; Lyulin, A. V.; Larin, S. V.; Gurtovenko, A. A.; Kenny, J. M.; Lyulin, S. V. Molecular Dynamics Simulations of Uniaxial Deformation of Thermoplastic Polyimides. *Soft Matter* **2016**, *12* (17), 3972–3981 DOI: 10.1039/C6SM00230G.

(69) Van Der Spoel, D.; Lindahl, E.; Hess, B.; Groenhof, G.; Mark, A. E.; Berendsen, H. J. C. GROMACS: Fast, Flexible, and Free. *J. Comput. Chem.* **2005**, *26* (16), 1701–1718 DOI: 10.1002/jcc.20291.

(70) Nazarychev, V. M.; Lyulin, A. V.; Larin, S. V.; Gurtovenko, A. A.; Kenny, J. M.; Lyulin, S. V. Molecular Dynamics Simulations of Uniaxial Deformation of Thermoplastic Polyimides. *Soft Matter* **2016**, *12* (17), 3972–3981 DOI: 10.1039/C6SM00230G.

(71) Berendsen, H. J. C.; Postma, J. P. M.; van Gunsteren, W. F.; DiNola, A.; Haak, J. R. Molecular Dynamics with Coupling to an External Bath. *J. Chem. Phys.* **1984**, *81* (8), 3684–3690 DOI: 10.1063/1.448118.

(72) Darden, T.; York, D.; Pedersen, L. Particle Mesh Ewald: An N·log(N) Method for Ewald Sums in Large Systems. *J. Chem. Phys.* **1993**, *98* (12), 10089 DOI: 10.1063/1.464397.

(73) Cisneros, G. A.; Karttunen, M.; Ren, P.; Sagui, C. Classical Electrostatics for Biomolecular Simulations. *Chem. Rev.* **2014**, *114* (1), 779–814 DOI: 10.1021/cr300461d.

(74) Hudzinskyy, D.; Lyulin, A. V.; Baljon, A. R. C.; Balabaev, N. K.; Michels, M. A. J. Effects of Strong Confinement on the Glass-Transition Temperature in Simulated Atactic Polystyrene Films. *Macromolecules* **2011**, *44* (7), 2299–2310 DOI: 10.1021/ma102567s.

(75) C. A. P. Joziasse, H. Veenstra, D. W. Grijpma and A. J. Pennings, Macromol. Chem. Phys., 1996, 197, 2219–2229.

(76) Sasanuma, Y.; Katsumata, S. Elucidation of Conformational Characteristics and Configurational Properties of poly((R)-3-hydroxybutyrate) by Ab Initio Statistical Mechanics. Polym. J. 2012, 45 (7), 727–737 DOI: 10.1038/pj.2012.203.

(77) Terada, M.; Marchessault, R. H. Determination of Solubility Parameters for poly(3-hydroxyalkanoates). *Int. J. Biol. Macromol.* **1999**, *25* (1–3), 207–215 DOI: 10.1016/S0141-8130(99)00036-7.

(78) Tsuji, H.; Sumida, K. Poly(L-Lactide): V. Effects of Storage in Swelling Solvents on Physical Properties and Structure of poly(L-hactide). *J. Appl. Polym. Sci.* **2001**, *79* (9), 1582–1589 DOI: 10.1002/1097-4628(20010228)79:9<1582::AID-APP60>3.0.CO;2-7.

(79) Meaurio, E.; Sanchez-Rexach, E.; Zuza, E.; Lejardi, A.; Sanchez-Camargo, A. del P.; Sarasua, J.-R. Predicting Miscibility in Polymer Blends Using the Bagley Plot: Blends with Poly(ethylene Oxide). *Polymer* **2017**, *113*, 295–309 DOI: 10.1016/j.polymer.2017.01.041.

(80) Zhang, W.; Gomez, E. D.; Milner, S. T. Predicting Flory-Huggins χ from Simulations. Phys. Rev. Lett. 2017, 119 (1), 17801 DOI: 10.1103/PhysRevLett.119.017801.

(81) Chen, G.-Q.; Wu, Q. The Application of Polyhydroxyalkanoates as Tissue Engineering Materials. Biomaterials 2005, 26 (33), 6565–6578 DOI: 10.1016/j.biomaterials.2005.04.036.

(82) Fox, T. G. *Bull. Amer. Phys. Soc.* **1956**, *1*, 123.

(83) Morita, H.; Tanaka, K.; Kajiyama, T.; Nishi, T.; Doi, M. Study of the Glass Transition Temperature of Polymer Surface by Coarse-Grained Molecular Dynamics Simulation. *Macromolecules* **2006**, *39* (18), 6233–6237 DOI: 10.1021/ma052632h.

(84) Baljon, A. R. C.; Williams, S.; Balabaev, N. K.; Paans, F.; Hudzinskyy, D.; Lyulin, A. V. Simulated Glass Transition in Free-Standing Thin Polystyrene Films. *J. Polym. Sci. Part B Polym. Phys.* **2010**, *48* (11), 1160–1167 DOI: 10.1002/polb.22005.

(85) Zhou, Y.; Milner, S. T. Short-Time Dynamics Reveals Tg Suppression in Simulated Polystyrene Thin Films. Macromolecules 2017, 50 (14), 5599–5610 DOI: 10.1021/acs.macromol.7b00921.

(86) Baljon, A. R. C.; Van Weert, M. H. M.; DeGraaff, R. B.; Khare, R. Glass Transition Behavior of Polymer Films of Nanoscopic Dimensions. *Macromolecules* **2005**, *38* (6), 2391–2399 DOI: 10.1021/ma048819a.

(87) Brodeck, M.; Alvarez, F.; Moreno, A. J.; Colmenero, J.; Richter, D. Chain Motion in Nonentangled Dynamically Asymmetric Polymer Blends: Comparison between Atomistic Simulations of PEO/PMMA and a Generic Bead–Spring Model. Macromolecules 2010, 43 (6), 3036–3051 DOI: 10.1021/ma902820a.

(88) Stevenson, C. S.; McCoy, J. D.; Plimpton, S. J.; Curro, J. G. Molecular Dynamics Simulations of Athermal Polymer Blends: Finite System Size Considerations. J. Chem. Phys. 1995, 103 (3), 1200–1207 DOI: 10.1063/1.469829.

(89) Stevenson, C. S.; Curro, J. G.; McCoy, J. D.; Plimpton, S. J. Molecular Dynamics Simulations of Athermal Polymer Blends: Comparison with Integral Equation Theory. J. Chem. Phys. 1995, 103 (3), 1208–1215 DOI: 10.1063/1.469830.

(90) White, R. P.; Lipson, J. E. G.; Higgins, J. S. New Correlations in Polymer Blend Miscibility. Macromolecules 2012, 45 (2), 1076–1084 DOI: 10.1021/ma202393f.

(91) Se, K.; Takayanagi, O.; Adachi, K. Dielectric Study of Miscibility in Weakly Segregated Polymer Blends. *Macromolecules* **1997**, *30* (17), 4877–4881 DOI: 10.1021/ma9703160.

(92) Faller, R. Correlation of Static and Dynamic Inhomogeneities in Polymer Mixtures: A Computer Simulation of Polyisoprene and Polystyrene. *Macromolecules* **2004**, *37* (3), 1095–1101 DOI: 10.1021/ma034991n.

(93) Harmandaris, V.; Doxastakis, M. Molecular Dynamics of Polyisoprene/polystyrene Oligomer Blends: The Role of Self-Concentration and Fluctuations on Blend Dynamics. J. Chem. Phys. 2013, 139 (3) DOI: 10.1063/1.4813019.

(94) Colby, R. H.; Lipson, J. E. G. Modeling the Segmental Relaxation Time Distribution of Miscible Polymer Blends: Polyisoprene/Poly(vinylethylene). *Macromolecules* **2005**, *38* (11), 4919–4928 DOI: 10.1021/ma0500741.

(95) Shenogin, S.; Kant, R.; Colby, R. H.; Kumar, S. K. Dynamics of Miscible Polymer Blends: Predicting the Dielectric Response. *Macromolecules* **2007**, *40* (16), 5767–5775 DOI: 10.1021/ma070503q.

(96) Liu, W.; Bedrov, D.; Kumar, S. K.; Veytsman, B.; Colby, R. H. Role of Distributions of Intramolecular Concentrations on the Dynamics of Miscible Polymer Blends Probed by Molecular Dynamics Simulation. *Phys. Rev. Lett.* **2009**, *103* (3), 37801 DOI: 10.1103/PhysRevLett.103.037801.

(97) Harmandaris, V. A.; Kremer, K.; Floudas, G. Dynamic Heterogeneity in Fully Miscible Blends of Polystyrene with Oligostyrene. *Phys. Rev. Lett.* **2013**, *110* (16), 165701 DOI: 10.1103/PhysRevLett.110.165701.

For Table of Contents use only.

Scale-Dependent Miscibility of Polylactide and Polyhydroxybutyrate: Molecular Dynamics Simulations

Artyom D. Glova, Stanislav G. Falkovich, Daniil I. Dmitrienko, Alexey V. Lyulin,

Sergey V. Larin, Victor M. Nazarychev, Mikko Karttunen, and Sergey V. Lyulin